

eingereicht/handed in: 03.08.2022  
angenommen/accepted: 19.12.2022

*Vivek Faldu, Oliver Beier, Andreas Pfuch, Kerstin Horn; INNOVENT e.V., Jena*

*Johannes Zender, Denis Wolf, Thomas Filler, Wolfgang Heinrich, Ulrike Winterwerber, Neysha Lobo Ploch; Ferdinand-Braun-Institut gGmbH, Leibniz-Institut für Höchstfrequenztechnik, Berlin*

## **Polymer surface functionalization using a new $\mu$ -wave driven atmospheric pressure plasma-jet device**

*A newly developed compact  $\mu$ -wave plasma source was utilized for activating the surfaces of several polymers. A remarkable improvement of the surface adhesion was achieved. The plasma-treated surfaces were investigated by AFM, XPS and surface free energy measurements. Also, actual adhesion improvements were evaluated by pull-off testing of paint-coatings applied after the plasma treatment. The plasma itself was characterized by optical emission spectroscopy, gas temperature determination as well as waste gas measurements.*

## **Oberflächenaktivierung von Polymeren mit Hilfe einer neuen Mikrowellen-Atmosphärendruck-Plasmaquelle**

*Eine neu entwickelte kompakte Plasmaquelle mit Mikrowellenanregung wurde hinsichtlich ihrer Eignung zur Vorbehandlung von Oberflächen untersucht. Dabei konnten deutliche Steigerungen der Haftfestigkeit von Lackierungen auf den vorbehandelten Oberflächen ermittelt werden. Als Analysemethoden kamen AFM- und XPS-Messungen an den vorbehandelten Bauteiloberflächen und Bestimmungen der freien Oberflächenenergie zum Einsatz. Ergänzt wurden die Untersuchungen durch Stempelabrisstests zur Bestimmung der Haftung von nachfolgend aufgetragenen Lackierungen. Das Plasma selbst wurde durch optische Emissionsspektroskopie, Gastemperaturbestimmungen sowie Abgasuntersuchungen charakterisiert.*

# Polymer surface functionalization using a new $\mu$ -wave driven atmospheric pressure plasma-jet device

V. Faldu, O. Beier, A. Pfuch., K. Horn, T. Filler, W. Heinrich, U. Winterwerber, N.L. Ploch, J. Zender, D. Wolf

## 1 INTRODUCTION

Nowadays, plasma processes, especially under ambient pressure conditions, have become an indispensable part of a variety of manufacturing processes for the activation of polymer materials. The basic effect behind this is that highly reactive plasma species in combination with high-energy UV radiation can make non-polar plastic surfaces accessible for subsequent bonding or printing by creating polar functional groups. On the one hand, this can be achieved by purely activating plasma processes with helpful reactive gases, in which in particular oxygen- or nitrogen-containing functional groups are created on the surface. On the other hand, layer-forming precursors or primer systems can be added into the plasma process, which leads to the formation of new thin adhesion promotion layers on the surface as well.

Looking at the multitude of different plasma systems, one first finds a great variety of large-area systems, mostly based on dielectric barrier discharges (DBD), e.g. [1, 2]. These systems are particularly suitable for the treatment of flat materials, e.g. textile woven and non-woven, certain sheet materials or plastic foils. Secondly, so-called jet plasma systems have increasingly entered the market in recent years, for example, by Plasmatreat, e.g. [3], Tigres, e.g. [4], neoplas, e.g. [5] or relyon [6] (all in Germany), vito, e.g. [7] (Belgium) or Tantec, e.g. [8] (Denmark). These systems are especially suited for local and selective treatments as well as for the treatment of three-dimensional materials. A comprehensive overview of different types of discharges as well as jet plasma devices and their relevance to adhesion can be found in [9].

This paper aims to introduce a new plasma system using microwave excitation and to present corresponding results in the field of plasma-based polymer surface activation. A major advantage of this system is its compact form factor. A controller unit integrated with the plasma source eliminates the need for additional external supply modules and resulting supply lines. Furthermore, this  $\mu$ -wave plasma source can be more advantageous than other conventional plasma systems in terms of power consumption and feasibility. In this paper, we investigate the influence of plasma treatment on the surface properties of pre-treated polymers. These results are supported by adhesion and optical emission spectroscopy measurements to determine the reactive species in the

plasma and by gas temperature measurements. Finally, results on waste gas production generated while  $\mu$ -wave plasma ignition will be presented.

## 2 COMPACT $\mu$ -WAVE PLASMA SOURCE

A new atmospheric pressure  $\mu$ -wave plasma source based on the plasma jet principle was developed by the Ferdinand-Braun-Institut (FBH), fig. 1. The device is a highly integrated low-temperature atmospheric plasma source that comprises a microwave power oscillator, a resonator, which excites the plasma, and the control circuit, all integrated into a single, miniaturized package, fig. 2.



*Figure 1: Compact  $\mu$ -wave atmospheric pressure plasma device, developed by the Ferdinand-Braun-Institut, the plasma jet is visible as a small plasma flame at the front-side of the source*

The microwave power oscillator which operates in the 2.45 GHz ISM band uses a gallium-nitride high electron mobility transistor (GaN HEMT) [10]. The high-frequency power generated by this transistor is coupled into a special  $\lambda/4$ -coaxial resonator which is responsible for both ignition and continuous stimulation of the plasma. With an external gas feed, the plasma is blown out at the front of the device. To maximize functionality and ease of use, the system has a built-in controller unit for easy plug-and-play applications and can be operated stand-alone or with an external PC. In addition, all supply voltages are provided by integrated DC/DC converters, requiring only a single external power supply of 48 V DC.

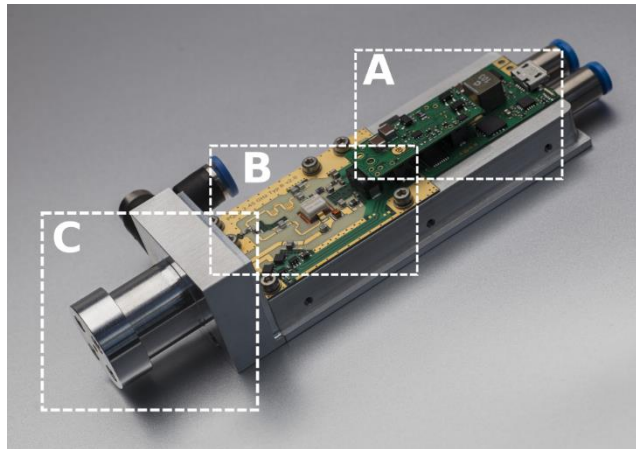


*Figure 2: The plasma source can be divided into three main sections: control unit (A), microwave power oscillator (B) and resonator (C)*

The  $\mu$ -wave plasma source is protected by a patent [11] and offers a number of advantages compared to more conventional sources. Due to the high frequency of the microwave power oscillator, the printed circuit board and the electrical components are very small, resulting in extremely compact device dimensions of 124 mm x 46 mm x 24.5 mm. Thanks to its small size and only three inputs for the 48 V DC power supply, water cooling and gas supply, it is easy to handle either as a stand-alone plasma tool or as part of a larger industrial system. The cooling water and the gas feed can be applied at the one-touch fittings mounted at the back of the device. Furthermore, since all structures needed to generate the plasma are integrated into the compact housing, this device has neither high voltage nor high frequency supply line which are known to be hard to handle and may radiate into the environment. Although water-cooling of the system is recommended to extract the heat generated during operation, the system can be adapted for active air cooling to enable easy integration into production lines. Another advantage of the compact  $\mu$ -wave plasma source is that the generated plasma is very homogeneous and has a low temperature which is very important for the treatment of temperature sensitive materials. This can be attributed to the high electron density and reduced ion mobility of microwave driven plasmas. Finally, the plasma source can be operated using different gases such as air, argon, oxygen or nitrogen without any hardware modifications. With different gases and flow rates, the temperature of the exhausted gas as well as the generated species of  $\text{NO}_x$  and ozone will be influenced. An optimum flow rate of 2 l/min with the use of air has been determined.

### 3 EXPERIMENTAL INVESTIGATIONS

Various polymer materials with dimensions of 50 x 50 mm<sup>2</sup> and substrate thicknesses of 2 to 3 mm (Rocholl GmbH) were used for the investigations. Polyamide nature (PA6, manufacture Sustaplast #26013), polypropylene nature (PP, manufacture Simona DWST #47846), polyethylene nature (LDPE, manufacture Simona PEW #68874 and HDPE, manufacture Simona HWST #68873), polycarbonate (PC, manufacture Makroform 099, #29678) and polymethyl methacrylate (PMMA, Röhm Plexiglas XT20070FF, #37191) were chosen as test polymers. Before treatment, all samples were pre-cleaned by hand with kimwipe tissues and isopropanol to remove any residues of release agents from the production process, after that the samples were sufficiently aired.

For plasma treatment, the samples were fixed on an x-y stage unit (Pasim Direktantriebe GmbH) and treated with different stage speeds (varying between 20 and 100 mm/sec) and different torch-substrate distances (varying between 2 and 10 mm), fig. 3. The samples were passed under the plasma source in a meandering manner with an offset of 1 mm, with only one system run. The used working gas was air, which flowed through the plasma system at 2 l/min and was adjusted by a variable area flowmeter of type Uniflux (VAF Fluid-Technik GmbH). The overall power consumption of the plasma source was about 90 W with at least 20 W plasma output.

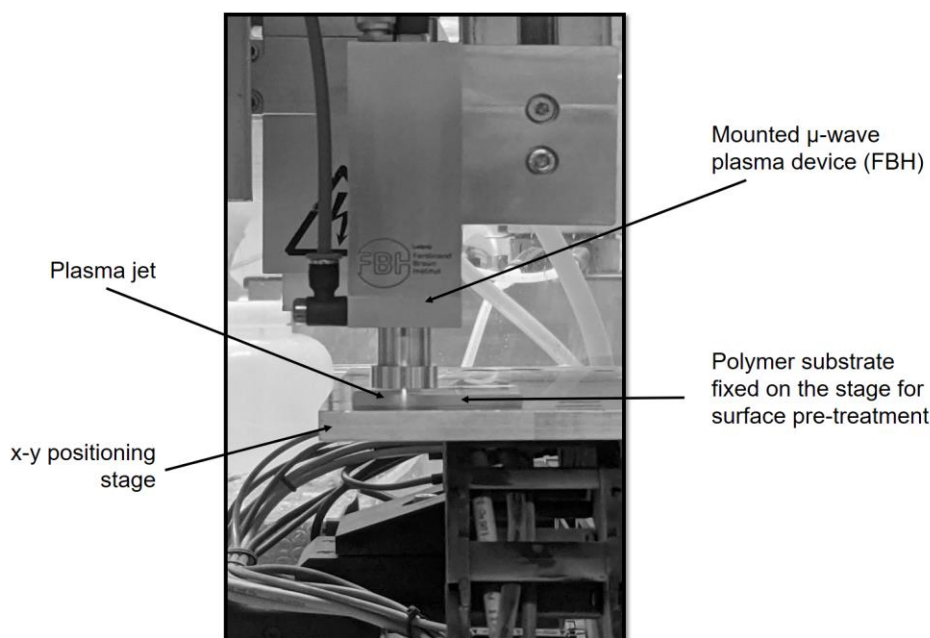


Figure 3: Image of the experimental setup depicting the  $\mu$ -wave plasma system, test sample and x-y stage

Immediately after the plasma treatments, the samples were painted with a polyurethane-based paint system (Mankiewicz H2O ALEXIT, decorative paint 341-34 920 C satin matt and hardener 345-24) that was applied with a spray gun. The lacquer was dried for 30 min at 80 °C and then for 24 h at room temperature. For the purpose of artificial aging of the applied lacquer, the samples treated in this way were stored in deionised water at 80 °C for 96 h, followed by drying of the samples for one day at room temperature. Afterwards, steel stamps (Erichsen GmbH & Co. KG) of 20 mm diameter were glued onto the lacquer surfaces that were sandblasted, treated with Pyrosil® and spray coated by a primer SuraLink21 (both Sura Instruments GmbH). The adhesive used was a ScotchWeld DP460 (2K epoxy from 3M Deutschland GmbH) which was cured for 3 h at 65 °C. With regard to the adhesion of lacquer – polymer, the adhesive bonding strength was quantitatively investigated by carrying out face pull-off tests. Ten bonding pairs were fabricated for each individual plasma parameter set for pull-off tests, and three samples each were reserved for analytical purposes. The pull-off tests were carried out using an inspect table 50 kN tensile testing machine (Hegewald & Peschke, Meß- und Prüftechnik GmbH) where the painted test specimen were fixed and the bonded steel stamps were pulled vertically upwards with a test speed of 5 mm/min.

Contact angle measurements and determination of the surface free energy on the plasma pre-treated polymer surfaces were carried out using an OCA15+ contact angle measuring device and the corresponding SCA 20 software (dataphysics GmbH), with each contact angle measurement value being averaged from ten measurements. As test liquids for contact angle measurements water, diiodomethane, ethylene glycol and thiodiglycol were used, and the drop volume was at 1 µl. All contact angle measurements were performed in a static regime at room temperature. The determination of the surface energy was performed according to the Owens, Wendt, Rabel and Kaelble (OWRK) model considering diiodomethane, ethylene glycol and thiodiglycol as test liquids. The surface roughness of the specimens was determined using an MFP 3D-Classic atomic force microscope (Asylum Research Oxford Instruments Inc.) over 10 x 10 µm<sup>2</sup> measuring areas. Here, each sample was analysed before and after plasma treatment at three different measuring points. The corresponding roughness values S<sub>a</sub> were determined according to EN ISO 25178 (software MarSurf MfM Premium, version: 7.4.8737). X-ray photoelectron spectroscopy (XPS) measurements for element-specific analysis of the polymer surfaces were performed using an Axis Ultra DLD (Kratos Analytical Ltd.) with a monochromatic X-ray source (Al Kα: 1468.6 eV).

To characterise the plasma source itself, plasma gas temperature measurements were done with air as the process gas and a flow of 2 l/min using a type K thermocouple and an YC-747U data logger (TC Mess- und Regelungstechnik GmbH). The species excited in the effluent were detected by optical emission spectroscopy measurements in the wavelength range between 200 and 1100 nm using an EMICON MC system (Plasus GmbH). For this, the

photosensor was aligned at a distance of 65 mm with a "view" directly into the plasma source.

Gas sensory measurements served as a further characterisation method to detect the number of certain reaction products of the plasma source. In a closed test chamber with a volume of approx. 3.3 m<sup>3</sup> and under constant gas circulation conditions, the plasma jet was operated with identical parameters as mentioned before. At a distance of about 45 cm from the plasma source, three gas sensing devices of the type Pac 8000 (Dräger Safety AG & Co. KGaA) were positioned, with sensitive characteristics to ozone (O<sub>3</sub>, 0 – 10 ppm), nitrogen dioxide (NO<sub>2</sub>, 0 – 50 ppm) and nitrogen monoxide (NO, 0 – 200 ppm). The measurement time was 720 seconds. It has to be emphasized that the cross sensitivity of the O<sub>3</sub> gas sensor towards NO<sub>2</sub> is about 55%. For the O<sub>3</sub> gas sensor towards NO, the NO gas sensor towards O<sub>3</sub>, NO<sub>2</sub> and the NO<sub>2</sub> gas sensor towards O<sub>3</sub>, NO no cross sensitivities are stated.

## 4 RESULTS

For all plasma-treated polymers, a significant increase in surface energy was observed. The values of the total surface energy of all plasma-treated samples were in the region of about 50 mN/m, see table 1. Whereas the dispersed part of the surface energy changed only within small margins, the polar component of the surface energy for all polymers increased substantially. Fig. 4 (left) compares the polar component of the surface energies determined on the basis of contact angle measurements and was carried out for both untreated and plasma-treated polymer samples. The increase in surface energy depends on the plasma parameters themselves and hence in the graph, the highest surface energy values for each polymer material are shown which correspond to the optimized plasma parameters stated in table 1. As can be seen, the polar component of the surface energy increased after plasma in most cases significantly and reached an average of approximately 10 mN/m. For PA6 we observed only a moderate increase due to the higher initial value for the untreated material. Furthermore, in the case of PA6 and PMMA, the spread of the measured surface energy values decreases substantially compared to the non-plasma-treated samples. In analogy, fig. 4 (right) shows the averaged adhesion values of the applied coating after aging, also for the process parameters where the highest increases could be measured. Significant improvements in the wettability of the surfaces as well as in the adhesion strength of the applied coatings have been observed for all plasma-treated polymer samples.

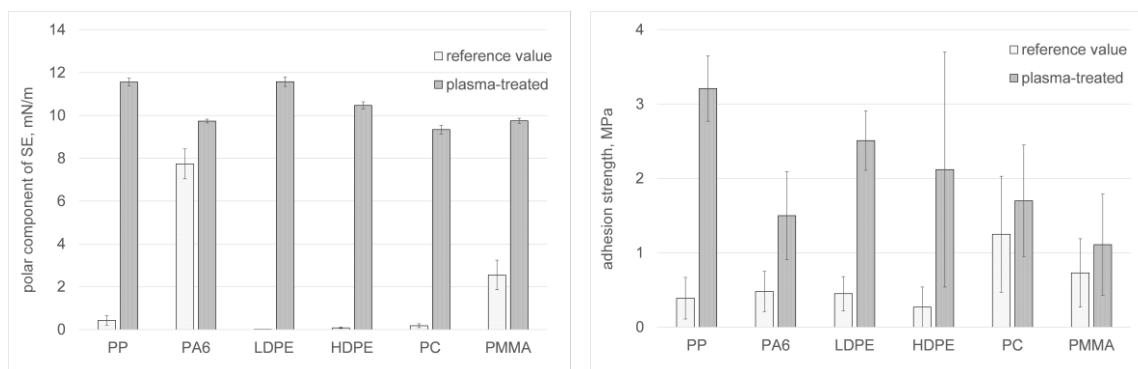


Figure 4: Polar component of the surface energy (left) and adhesion strength values (right) for plasma pre-treated polymer substrates, the area for contact angle measurements was about 50 x 50 mm<sup>2</sup>, the glued surface area had a diameter of 20 mm, the number of measurements per each polymer was 10

The increase of the surface energy corresponds well with literature data based on atmospheric plasma treatments (certain jet plasma systems as well as DBD systems) on different polymers like PP [12 - 14, 3], PA6 [15 - 17, 3], LDPE [18 - 21], HDPE [22, 23, 17, 3], PC [24 - 26] and PMMA [27 - 30]. Furthermore, the measured tensile strength values are comparable with previous results that have been observed by using the same test equipment and with samples treated by certain atmospheric pressure plasma as well as flame procedures [31].

Table 1 compares the surface energy values and the adhesion strength values with the corresponding process parameters. With a view especially on the process parameters given in table 1 and considering previously obtained results [31, 32], it has to be mentioned that there is not necessarily a strong correlation between high surface energy and high adhesion strength. Instead, it is confirmed that adhesion tests rather than surface energy measurements should be used to assess the effectiveness of a pre-treatment procedure.

polymer	surface energy, mN/m					adhesion strength, MPa		
	untreated reference		μ-wave plasma		corresponding treatment	untreated reference		corresponding treatment
	total	polar	total	polar		value	value	
PP	30.1 ± 1.0	0.4 ± 0.2	50.5 ± 0.3	11.6 ± 0.2	H = 2 mm v = 20 mm/s	0.4 ± 0.3	3.2 ± 0.4	H = 2 mm v = 100 mm/s
PA6	47.8 ± 1.2	7.7 ± 0.7	52.9 ± 0.2	9.7 ± 0.1	H = 2 mm v = 50 mm/s	0.5 ± 0.3	1.5 ± 0.6	H = 2 mm v = 20 mm/s
LDPE	32.8 ± 0.6	0.0 ± 0.0	50.1 ± 0.4	11.6 ± 0.2	H = 2 mm v = 20 mm/s	0.5 ± 0.2	2.5 ± 0.4	H = 2 mm v = 20 mm/s
HDPE	34.8 ± 0.6	0.1 ± 0.0	49.5 ± 0.3	10.5 ± 0.2	H = 2 mm v = 20 mm/s	0.3 ± 0.3	2.1 ± 1.6	H = 5 mm v = 100 mm/s
PC	45.8 ± 0.7	0.2 ± 0.1	52.5 ± 0.4	9.3 ± 0.2	H = 2 mm v = 20 mm/s	1.3 ± 0.8	1.7 ± 0.8	H = 5 mm v = 20 mm/s
PMMA	44.8 ± 0.9	2.6 ± 0.7	50.2 ± 0.2	9.8 ± 0.1	H = 2 mm v = 100 mm/s	0.7 ± 0.5	1.1 ± 0.7	H = 2 mm v = 50 mm/s

Table 1: Results of surface energy and adhesion strength measurements, the area for contact angle measurements was about 50 x 50 mm<sup>2</sup>, the glued surface area had a diameter of 20 mm, the number of measurements per each polymer was 10

The observed improvements in adhesion strength can be attributed to the creation of new functional groups on the polymer surface. To verify this, XPS measurements were carried out for all plasma-treated polymers. Fig. 5 represents the results of such measurements exemplary for the PA6 material. In this matter especially, the measurement of XPS detail spectra of the carbon peak for treated material and its comparison to the untreated material is of interest due to the slight shift in binding energy for the carbon signal. Namely, whereas for the pure C-C single bond a binding energy of 284,6 eV will be observed, for the C-N bond, the C-O bond, the O=C-N bond and the C=O bond 285,6 eV, 286,4 eV, 287,5 eV and 288,5 eV will be expected, respectively. Fig. 5 (left) shows such a detailed spectrum for plasma-treated PA6 material together with the results of the fitting procedure for the C-C bond and these new bonding states. Thus, the investigations of the bonding states of carbon allow concluding new functional groups that lead to stronger physical bonds with the subsequently applied adhesive system.

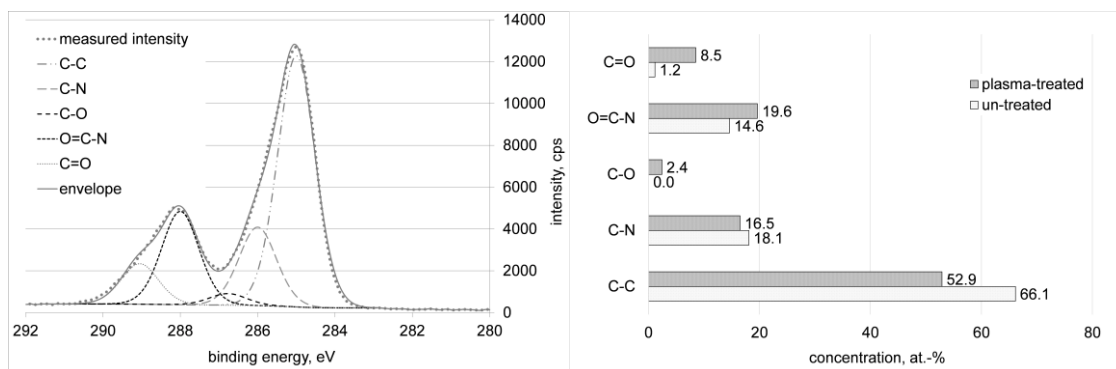


Figure 5: XPS-detail spectrum of the carbon C1s signal (left) and amount (in at. %) of functional groups obtained on a plasma-treated PA6 polymer surface compared to pure C-C bonds (right)

It can be seen from fig. 5 (right) that the relative amount of single carbon bonds on the surface decreases significantly due to the plasma treatment, while the amount of carbon-nitrogen and carbon-oxygen single bonds increases significantly. Similarly, the relative proportion of carboxylic acid, amide groups and carbon-oxygen double bonds increases. Considering the total elemental concentrations of the PA6 reference and after plasma treatment, a decrease of carbon C1s from 77.4 at.-% to 66.1 at.-% and an increase of oxygen O1s from 11.8 at.-% to 20.7 at.-% as well as of nitrogen N1s from 10.2 at.-% to 13.1 at.-% were measured.

In the context of adhesion processes, mechanical bond types also play an important role. In this respect, the consideration of roughness is an interesting point. Looking at the measured surface topographies of the plasma-treated samples, a different picture emerges. Fig. 6 shows two AFM topography measurements, measured on PA6 samples. In this case, a significant roughening of the surface on the nanometer scale is observed.

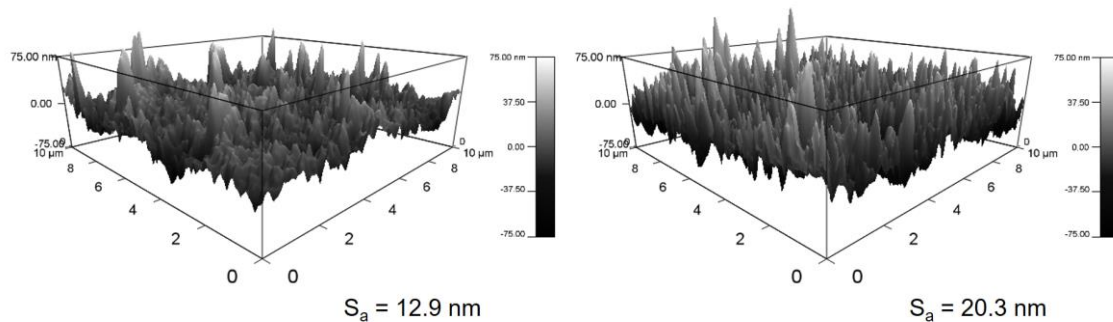


Figure 6: AFM topography measurements on a PA6 surface, reference (left), plasma-treated (with 20 mm/s velocity, 2 mm distance) (right), the measurement area was  $10 \times 10 \mu\text{m}^2$

Fig. 7 (left) illustrates the change in the surface roughness of all investigated polymers due to the  $\mu$ -wave plasma treatment. Each polymer was treated using its optimal process parameters (see table 1, adhesion strength measurements), i.e. the parameter set which obtained the highest surface adhesion.

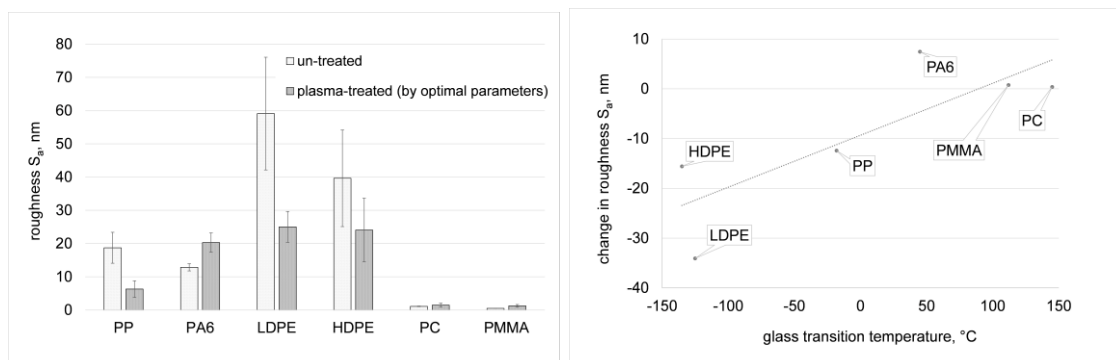


Figure 7: Roughness values  $S_a$  of un-treated and plasma-treated polymer surfaces (left), the measurement area for determination of the roughness was  $10 \times 10 \mu\text{m}^2$ , the number of roughness measurements per each polymer was 3, the plasma treatment was applied in accordance with the parameters given in table 1 for the best adhesion strength values, the change of the surface roughness in dependence on typical glass transition temperatures [33, 34] is shown on the right side

It was observed that the roughness increases for the PA6, PC and PMMA surface after plasma treatment but tends to decrease for PP, LDPE and HDPE. Taking into account the measured adhesion values for the investigated polymers it has to be mentioned that we did not find a strong correlation

between the surface roughness and the adhesion values obtained. Nevertheless, a possible explanation for the changes in roughness in both directions, both as roughening and levelling, could be the different glass transition temperatures of the used polymers. Fig. 7 (right) shows the dependence of the change in roughness on typical glass temperature values [33, 34] of the used polymers indicating this possible correlation.

It can be seen that the polymers with negative glass transition temperature all show a decrease in the roughness after plasma treatment. The heat impact of the plasma might macerate the surface of these polymers leading to a flattening of the surface. On the other hand, PA6, PMMA, and PC all have significantly higher glass transition temperatures, where the roughening may occur due to the direct plasma impact (electrons, ions, excited species and irradiation). With changes in the optimal treatment parameters for the different polymers, the thermal impact of the  $\mu$ -wave plasma on each polymer surface also changes to some extent. The highest gas temperature, measured with a thermocouple, see fig. 9, is only about 70 °C for the most intense plasma parameter ( $h = 2$  mm;  $v = 20$  mm/s). Hence, it can be expected that the maximum temperature at the polymer surfaces does not exceed this value.

Regarding the creation of new functional groups at the polymer surface, the reactive species in the plasma jet and their interaction with the polymer surface play an essential role. Optical emission spectroscopy was used to determine the reactive species in the plasma by aligning the photo sensor directly along the plasma jet axis (view into the plasma source). Fig. 8 shows three spectra taken at different radial distances from the center of the plasma jet. At first glance, one can see the dramatic loss of intensity when the photo sensor is moved away from the axis of the plasma jet. Moving the sensor 1.1 mm away, the signal intensity of the most prominent emissions decreases already to about 20 %, in comparison to the intensity of the plasma center. Due to this, a grid spacing distance of 1 mm was chosen, to get a uniform plasma treatment over the whole polymer area. Focusing on the species excited in the air plasma center, emissions of nitric oxides (NO), the second positive system ( $N_2$  SPS) and first positive system ( $N_2$  FPS) of nitrogen molecules, the first negative system of the nitrogen molecular ions ( $N_2^+$ ) and atomic oxygen (O) were detected.

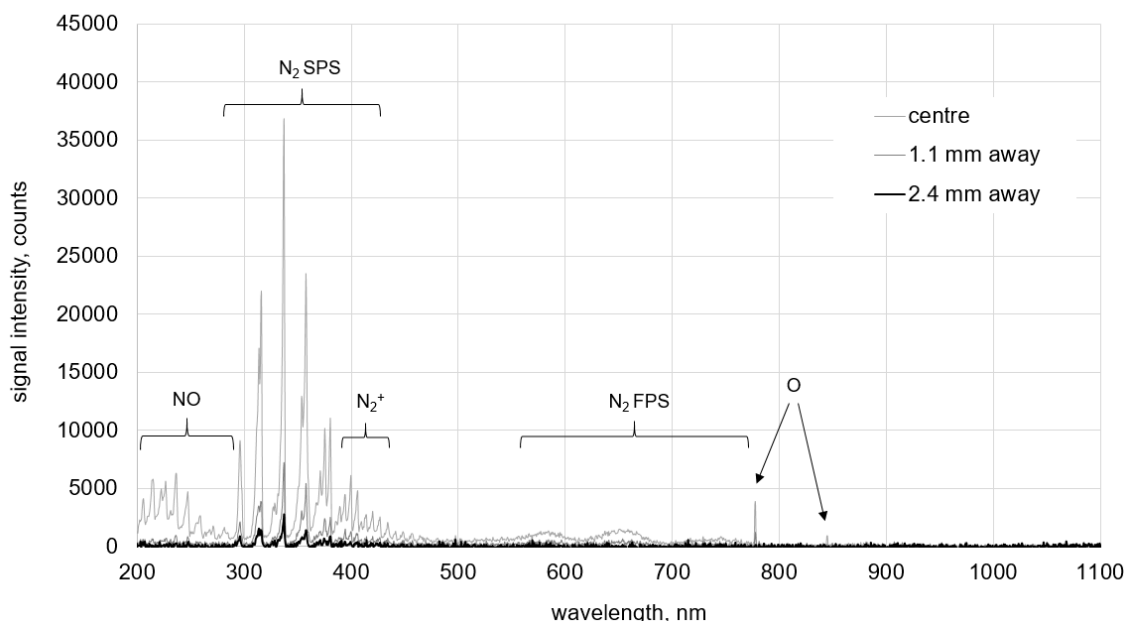


Figure 8: Optical emission spectra of the gas excited by the  $\mu$ -wave plasma

Besides a direct interaction of excited electrons from the plasma with the polymer surfaces and following reactions with  $O_2$  and  $N_2$  (surrounding air), also the observed oxygen and nitrogen containing reactive species can play an important role with regard to the measured chemical changes on the polymer surface (see XPS results from fig. 5). Especially the excited atomic oxygen (O) states are expected, to increase the concentration of C-O and C=O bondings and the overall oxygen concentration, as observed for the plasma treated PA surfaces. Also the measured increase of nitrogen containing functional groups can be at least partially attributed to interactions with the excited  $N_2$ ,  $N_2^+$  and NO states.

The observed nitrogen-containing species and emission systems (NO,  $N_2$ ,  $N_2^+$ ) are very similar to descriptions from Deng et al. for a direct current (dc) plasma jet at atmospheric pressure [35]. A plasma generated by air discharge and electrical current of 14 mA (stable discharge mode) showed in the active plasma zone the same emission systems. In contrast, lines of atomic oxygen were not present in this type of plasma. Also a commercial plasma jet, the MEF (Tigres GmbH) with a dc pulsed electric barrier discharge and air as process gas emits very similar irradiation, like the  $\mu$ -wave plasma source. Emissions of NO,  $N_2$ ,  $N_2^+$  and O could be found and additionally small intensities of OH as well as Cu, which was correlated to the metallic (brass) high voltage electrode [36].

The group of Lommatzsch et al. investigated the relaxing plasma of a pulsed arc plasma jet (Plasmatrete GmbH) with air as a process gas and excitation frequencies between 17 and 22 kHz [37]. Besides NO,  $N_2$  SPS and O, like for

the  $\mu$ -wave plasma system, a continuum emission of  $\text{NO}_2$  molecules in the wavelength range of 450 – 800 nm could be also identified. Likewise, other groups confirmed the observation of  $\text{NO}_2$  continuum emissions for this kind of arc plasma jet [38, 39].

With a view on air driven atmospheric plasma jets also completely different spectra or ratios of excited species can be found, in comparison to the plasma sources described before and the microwave discharge. In the descriptions of Ahn et al., where a plasma jet from a micro nozzle array is formed, the optical emission spectrum is dominated by excited oxygen atoms at 777 and 845 nm and molecules above 500 nm, which were assigned to  $\text{N}_2$  SPS and  $\text{N}_2$  FPS [40].

The simultaneous measurement of the gas concentration with three gas sensor devices ( $\text{O}_3$ ,  $\text{NO}$ ,  $\text{NO}_2$ ) showed the following behavior for the investigated plasma source. Over the measurement time of 720 seconds, no  $\text{NO}$  was detected. For  $\text{O}_3$  and  $\text{NO}_2$ , on the other hand, a continuous increase in gas concentration was detected, with a transition into a saturation state starting at about 600 seconds after switching on the plasma device. The maximum gas concentrations were found to be 0.98 ppm for  $\text{O}_3$  and 2.20 - 2.26 ppm for  $\text{NO}_2$ . One possible explanation for the absence of  $\text{NO}$  could be the relatively low temperatures (see next section – thermocouple measurements), compared to other plasma jet sources. Using the same experimental setup with a commercial pulsed arc plasma jet (Openair-Plasma® - Nozzle PFW10, Plasmatrete GmbH), air as a process gas and standard electrical parameters (frequency: 21.0 kHz, voltage: 280 V, current: 9.1 A) the maximum gas concentrations were measured to be 93.5 ppm for  $\text{NO}$ , 5.85 ppm for  $\text{O}_3$  and 14.9 ppm for  $\text{NO}_2$ . The group of Malik et al. investigated an atmospheric pressure surface discharge at different temperatures of the electrodes (20 °C to 420 °C) and observed a similar trend regarding the  $\text{NO}$  gas concentrations [41]. At 20 °C and 120 °C, no  $\text{NO}$  (detection limit: 100 ppm) and from 220 °C onwards rising  $\text{NO}$  concentrations were detected. Vice-versa, the  $\text{O}_3$  concentrations decreased with rising electrode temperatures and were below the detection limit of  $\geq 220$  °C. Formed  $\text{NO}$  could be further oxidized to  $\text{NO}_2$  or higher oxidation states by interaction with  $\text{O}_3$  or  $\text{O}$ , which are also described as fast reactions at low / room temperature. On the other hand, high plasma temperatures (e.g. in arc plasmas) can destroy  $\text{O}_3$  and hence minimize the  $\text{NO}$  to  $\text{NO}_2$  conversion [41].

The optimal process parameters in table 1 are directly related to the temperature of the plasma gas. Keeping this in mind, appropriate thermocouple measurements were done, see fig. 9. Directly at the nozzle outlet, relatively high gas temperatures of about 200 °C were observed in the static regime, at an air gas flow through the plasma source of 2 l/min. At a distance of about 7-8 mm from the nozzle outlet, the gas temperature drops to less than 100 °C. In a dynamic regime, a maximum temperature of approx. 70 °C was measured for the parameter with the highest intensity ( $h = 2$  mm;  $v = 20$  mm/s). With increasing distance as well as with higher velocity, the maximal measured temperatures drop in each case to the range of approx. 50 °C. Based on these

investigations, the  $\mu$ -wave plasma source can be efficiently used for the plasma treatment of thermally sensitive materials.

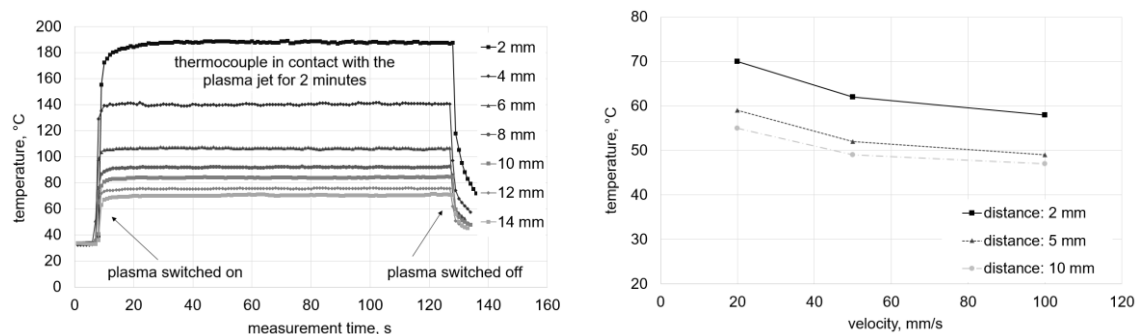


*Figure 9: Temperature measurements in the plasma jet for different distances from the nozzle – statically (left) and dynamically for different treatment velocities between 20 – 100 mm/s (maximal observed temperature values, right)*

## 5 SUMMARY

In summary, a new compact atmospheric pressure  $\mu$ -wave plasma source based on the plasma-jet principle has been presented for use both as a stand-alone device and as part of an industrial system. It can be clearly stated from the experimental observations that the  $\mu$ -wave plasma source is very effective and perfectly suitable for improving the surface energies and the adhesive properties of all the examined polymers. Despite a large increase in surface energies of PC and PMMA through the  $\mu$ -wave plasma treatment, the adhesion strength of these materials increased only moderately, which indicates that the other factors like surface roughness and chemical compositions on the surfaces are important factors supporting the adhesion mechanism. The optical emission spectroscopy revealed the exciting species present inside the plasma and also provided information on the effective area of the plasma jet for the treatment of polymer materials. Precise thermal measurements of the  $\mu$ -wave plasma jet along the central plasma axis for static and dynamic plasma conditions show that the  $\mu$ -wave plasma source can be efficiently used for the plasma treatment of thermally sensitive materials. A mild concentration of  $O_3$  and  $NO_2$  was detected during the  $\mu$ -plasma ignition, while no indication of  $NO$  generation was observed.

Thus, the presented new compact  $\mu$ -plasma source is excellently suited for the selective and local functionalization of polymer surfaces for adhesion improvement.

## REFERENCES

[1]	Leroux, F.; Perwuelz, A.; Campagne, C.; et al.	Atmospheric air-plasma treatments of polyester textile structures  Journal of Adhesion Science and Technology, 20:9, pp. 939-957  DOI: 10.1163/156856106777657788
[2]	Cernak, M.; C ernakova, L.; Hudec, I.; et al.	Diffuse Coplanar Surface Barrier Discharge and its applications for in-line processing of low-added-value materials  The European Physical Journal Applied Physics 47 (2009) 22806  DOI: 10.1051/epjap/2009131
[3]	Noeske, M.; Degenhardt, J.; Strudthoff, S.; et al.	Plasma jet treatment of five polymers at atmospheric pressure: surface modifications and the relevance for adhesion  International Journal of Adhesion & Adhesives 24 (2004) pp. 171–177  DOI: 10.1016/j.ijadhadh.2003.09.006
[4]	Kumar, S.; Abhishek, G.; Ullattil, A.; et al.	Effect of atmospheric pressure plasma treatment for repair of polymer matrix composite for aerospace applications  Journal of Composite Materials, 50(11), pp. 1497–1507  DOI: 10.1177/0021998315594230
[5]	Reuter, S.; v. Woedtke, T.; Weltmann, K.- D.	The kINPen—a review on physics and chemistry of the atmospheric pressure plasma jet and its applications  <i>Journal of Physics D: Applied Physics</i> 51 (2018) 233001 (51pp)  DOI: 10.1088/1361-6463/aab3ad
[6]	Korzec, D.; Burger, D.; Nettesheim, S.	Plasmaaktivierung von Rolle zu Rolle  Adhäsion KLEBEN & DICHTEN, 59(3), pp. 26–31  DOI: 10.1007/s35145-015-0514-5

[7]	Verheyde, B.; Rombouts, M.; Vanhulsel, A.; et al.	Influence of surface treatment of elastomers on their frictional behaviour in sliding contact Wear, 266(3-4), pp. 468–475 DOI: 10.1016/j.wear.2008.04.040
[8]	Van Steenacker, P.	Allseitig aktiviert bei Atmosphärendruck Adhäsion KLEBEN & DICHTEN, 57(10), pp. 30–33 DOI: 10.1365/s35145-013-0399-0
[9]	Thoma, M.; Mittal, K.L.	Atmospheric Pressure Plasma Treatment of Polymers Relevance to Adhesion Edts.: M. Thomas, K.L. Mittal, Scrivener Publishing LLC, Salem, Massachusetts, 2013 ISBN 978-1-118-59621-0 DOI: 10.1002/9781118747308
[10]	Lossy, R.; Blanck, H.; Würfl, J.	Sputtered Iridium Gate Module for GaN HEMT with Stress Engineering and High Reliability Int. Conf. on Compound Semiconductor Manufacturing Technology (CS ManTech 2014), Denver, Colorado, USA, May 19 <sup>th</sup> - 22 <sup>nd</sup> , pp. 193-196
[11]	Wolf, D.	Resonator und Leistungoszillator zum Aufbau einer integrierten Plasmaquelle sowie deren Verwendung German patent No. DE 10 2020 100 872 B4, (2021)
[12]	Oravcova, A.; Hudec, I.	The Influence of Atmospheric Pressure Plasma Treatment on Surface Properties of Polypropylene Films Acta Chimica Slovaca, Vol.3, No.2, 2010, pp. 57 - 62
[13]	Leroux, F.; Campagne, C.; Perwuelz, A.; et al.	Polypropylene film chemical and physical modifications by dielectric barrier discharge plasma treatment at atmospheric pressure Journal of Colloid and Interface Science 328 (2008) pp. 412–420 DOI: 10.1016/j.jcis.2008.09.062

[14]	Kehrer, M.; Rottensteiner, A.; Hartl, W.; et al.	Cold atmospheric pressure plasma treatment for adhesion improvement on polypropylene surfaces Surface & Coatings Technology 403 (2020) 126389 DOI: 10.1016/j.surfcoat.2020.126389
[15]	Karoly, Z.; Kalacska, G.; Zsidai, L.; et al.	Improvement of Adhesion Properties of Polyamide 6 and Polyoxymethylene-Copolymer by Atmospheric Cold Plasma Treatment Polymers 2018, 10, 1380 DOI: 10.3390/polym10121380
[16]	Schäfer, J.; Hofmann, T.; Holtmannspötter, J.; et al.	Atmospheric-pressure plasma treatment of polyamide 6 composites for bonding with polyurethane Journal of Adhesion Science and Technology, 29:17, pp. 1807-1819 DOI: 10.1080/01694243.2015.1037380
[17]	Al-Maliki, H.; Kalacska, G.	The effect of atmospheric DBD plasma on surface energy and shear strength of adhesively bonded polymer Hungarian Agricultural Engineering N° 31/2017 pp. 52-58 DOI: 10.17676/HAE.2017.31.52
[18]	Fombuena V.; García- Sanoguera, D.; Sánchez- Nacher, L.; et al.	Optimization of atmospheric plasma treatment of LDPE films: Influence on adhesive properties and ageing behaviour Journal of Adhesion Science and Technology, 28(1), pp. 97-113 DOI: 10.1080/01694243.2013.847045
[19]	Sanchez- Nacher, L.; Garcia- Sanoguera, D.; Fenollar, O.; et al.	Improvement of adhesion properties of low density polyethylene (LDPE) substrate using atmospheric plasma AIP Conference Proceedings 1255, 323 (2010) DOI: 10.1063/1.3455623
[20]	Navaneetha Pandiyaraj, K.; Arun Kumar., A.; RamKumar, M.C.; et al.	Effect of cold atmospheric pressure plasma gas composition on the surface and cyto-compatible properties of low density polyethylene (LDPE) films Current Applied Physics 16 (2016) 784e792 DOI: 10.1016/j.cap.2016.04.014

[21]	Novak, I.; Steviar, M.; Popelka, A.; et al.	Surface modification of polyethylene by diffuse barrier discharge plasma Polymer Engineering and Science 53 (2013) pp. 516-523 DOI: 10.1002/pen.23280
[22]	Guragain, R.P.; Baniya, H.B.; Dhungana, S.; et al.	Characterization Of Dielectric Barrier Discharge (DBD) Produced In Air At Atmospheric Pressure And Its Application In Surface Modification Of High-Density Polyethylene (HDPE) Journal of Technological and Space Plasmas, Vol. 1, Issue 1 (2020) DOI: 10.31281/jtsp.v1i1.11
[23]	Freire de Medeiros Neto, J.; Alves de Souza, I.; Feitor, M.C.; et al.	Study of High-Density Polyethylene (HDPE) Kinetics Modification Treated by Dielectric Barrier Discharge (DBD) Plasma Polymers 2020, 12, 2422 DOI: 10.3390/polym12102422
[24]	Kelar, J.; Shekargoftar, M.; Krupolec, R.; et al.	Activation of polycarbonate (PC) surfaces by atmospheric pressure plasma in ambient air Polymer Testing (2018) DOI: 10.1016/j.polymertesting.2018.03.027
[25]	Kostov, K.G.; Hamia, Y.A.A.; Mota, R.P.; et al.	Treatment of polycarbonate by dielectric barrier discharge (DBD) at atmospheric pressure Journal of Physics: Conference Series 511 (2014) 012075 DOI: 10.1088/1742-6596/511/1/012075
[26]	Shrestha, A.K.; Dotel, B.S.; Dhungana, S.; et al.	Surface modification of polycarbonate for improvement of wettability using mesh electrode at atmospheric pressure discharge at 50Hz National Symposium on Emerging Plasma Techniques for Materials Processing and Industrial Applications (N-SEPMI 2014)
[27]	Homola, T.; Matousek, J.; Hergelova, B.; et al.	Activation of poly(methyl methacrylate) surfaces by atmospheric pressure plasma Polymer Degradation and Stability 97 (2012) 886e892 DOI: 10.1016/j.polymdegradstab.2012.03.029

[28]	Rezaei, F.; Shokri, B.; Sharifan, M.	Atmospheric-pressure DBD plasma-assisted surface modification of polymethylmethacrylate: A study on cell growth/proliferation and antibacterial properties Applied Surface Science 360 (2016) pp. 641–651 DOI: 10.1016/j.apsusc.2015.11.036
[29]	Fang, Z.; Liu, Y.; Liu, K.; et al.	Surface modifications of polymethylmetacrylate films using atmospheric pressure air dielectric barrier discharge plasma Vacuum 86 (2012) pp. 1305-1312 DOI: 10.1016/j.vacuum.2011.11.021
[30]	Abdel-Fattah, E.	Surface Activation of Poly(Methyl Methacrylate) with Atmospheric Pressure Ar + H <sub>2</sub> O Plasma Coatings 2019, 9, 228 DOI: 10.3390/coatings9040228
[31]	Pfuch, A.; Schiemann, S.; Erler, I.; et al.	Tensile adhesion test for paint Kunststoffe International 3/2007, pp.16-20
[32]	Pfuch, A.; Beier, O.; Gitter, U.; et al.	CFK-Bauteile: Einfluss physikalischer Vorbehandlungen auf die Verklebung Galvanotechnik 12/2021, pp. 1606-1613
[33]	dos Santos, W.N.; de Sousa, J.A.; Gregorio Jr., R.	Thermal conductivity behaviour of polymers around glass transition and crystalline melting temperatures Polymer Testing 32 (2013) pp. 987–994 DOI: 10.1016/j.polymertesting.2013.05.007
[34]	Grigorescu, R.M.; Grigore, M.E.; Iancu, L.; et al.	Waste Electrical and Electronic Equipment: A Review on the Identification Methods for Polymeric Materials Recycling 2019, 4, 32 DOI: 10.3390/recycling4030032
[35]	Deng, X. L.; Nikiforov, A. Y.; Vanraes, P.; et al.	Direct current plasma jet at atmospheric pressure operating in nitrogen and air Journal of Applied Physics 113, 023305 (2013) DOI: 10.1063/1.4774328

[36]	Horn, K.; Beier, O.; Wiegand, C.; et al.	Screening test of a new pulsed Plasma Jet for medical application Plasma Medicine 7, 2 (2017), pp. 133-145 DOI: 10.1615/PlasmaMed.2017019094
[37]	Lommatzsch, U.; Pasedag, D.; Baalmann, A.; et al.	Atmospheric Pressure Plasma Jet Treatment of Polyethylene Surfaces for Adhesion Improvement Plasma Processes and Polymers 4 (2017), pp. 1041-1045 DOI: 10.1002/ppap.200732402
[38]	Dowling, D. P.; O'Neill, F. T.; Langlais, S. J.; et al.	Influence of dc Pulsed Atmospheric Pressure Plasma Jet Processing Conditions on Polymer Activation Plasma Processes and Polymers 8 (2011), pp. 718-727 DOI: 10.1002/ppap.201000145
[39]	Carton, O.; Salem, D. B.; Pulpytel, J.; et al.	Improvement of the Water Stability of Plasma Polymerized Acrylic Acid/MBA Coatings Deposited by Atmospheric Pressure Air Plasma Jet Plasma Chemistry and Plasma Processing, 35 (2015), pp. 819–829 DOI: 10.1007/s11090-015-9634-9
[40]	Ahn, H. J.; Kim, K. I.; Kim, G.; et al.	Atmospheric-Pressure Plasma Jet Induces Apoptosis Involving Mitochondria via Generation of Free Radicals PLoS ONE 6(11): e28154, (2011) DOI: 10.1371/journal.pone.0028154
[41]	Malik, M. A.; Jiang, C.; Heller, R.; et al.	Ozone-free nitric oxide production using an atmospheric pressure surface discharge – A way to minimize nitrogen dioxide co-production Chemical Engineering Journal 283 (2016), pp. 631-638 DOI: 10.1016/j.cej.2015.07.092

### Bibliography

DOI 10.3139/O999.01022023  
Zeitschrift Kunststofftechnik / Journal of Plastics  
Technology 19 (2023) 2; page 52–72  
© Carl Hanser Verlag GmbH & Co. KG  
ISSN 1864 – 2217

**Keywords:**

**microwave plasma**, atmospheric pressure plasma, plasma characterisation, polymer surface functionalisation, adhesion improvement

**Stichworte:**

**Mikrowellenplasma**, Atmosphärendruckplasma, Plasmacharakterisierung, Oberflächenfunktionalisierung von Kunststoffen, Haftungsverbesserung

**Autor / author**

Vivek Faldu  
Innovent e.V.  
Prüssingstr. 27B  
07745 Jena - Germany

E-Mail: vf@innovent-jena.de  
Phone: +49 (0) 3641 282510

**Herausgeber / Editors****Europa / Europe**

Prof. Dr.-Ing. habil. Bodo Fiedler  
Institute of Polymers and Composites  
University of Technology Hamburg  
Denickestr. 15  
21073 Hamburg  
Germany  
Phone: +49 (0)40 42878 3038  
E-Mail: fiedler@kunststofftech.com

Prof. Dr.-Ing. Reinhard Schiffers  
Institute of Product Engineering  
University of Duisburg-Essen  
Lotharstr. 1, MA 222  
47057 Duisburg  
Germany  
Phone: +49 (0)203 379 2500  
E-Mail: schiffers@kunststofftech.com

**Amerika / The Americas**

Prof. Prof. hon. Dr. Tim A. Osswald  
Polymer Engineering Center, Director  
University of Wisconsin-Madison  
1513 University Avenue  
Madison, WI 53706  
USA  
Phone: +1 608 Experten aus Forschung und  
Industrie, gelistet unter 263 9538  
E-Mail: osswald@enr.wisc.edu

**Verlag / Publisher**

Carl-Hanser-Verlag GmbH & Co. KG  
Jo Lendle, Oliver Rohloff  
Geschäftsführer  
Kolbergerstraße 22  
81679 München  
Germany  
Phone: +49 (0)89/99830-0  
E-Mail: info@hanser.de

**Redaktion / Editorial Office**

Dr.-Ing. Eva Bittmann  
Janina Mittelhaus, M.Sc.  
E-Mail: editor@plasticseng.com.

**Beirat / Advisory Board**

Experts from research and industry, listed under  
www.kunststofftech.com / www.plasticseng.com